1st National Applied Mechanisms & Robotics Conference, Cincinnati, Ohio, Nov. 5-8, 1989, 89AMR-3A-3, Volume I.

AUTONOMOUS RECTILINEAR MOTION PLANNING
Part I: The Geometry of the Wrist Workspace with A Single Circular Obstacle

Meng-Dar Shieh
Research Assistant

Joseph Duffy
Graduate Research Professor
Department of Mechanical Engineering
Director
Center for Intelligent Machines and Robotics
University of Florida
Gainesville, Florida 32611

ABSTRACT

This is the first of a series of papers which develop a time efficient algorithm for the rectilinear motion of a point in the end effector of a planar 3R manipulator with multiple circular obstacles in the workspace. The algorithm can be used to guide 3R manipulators and a snake robot which can be modeled by a sequence of 3R manipulators through horizontal pipes with circular cross-sections. Further, the algorithm can be modified to guide Puma and T^{3}776 robots through horizontal pipes with circular cross-sections. The time of execution of the algorithm for a single 3R manipulator using the Silicon Graphics 4D system for single and multiple obstacles is within 1 second and 3 seconds respectively. In this first of the sequence of papers, the geometry of the wrist workspace with a single obstacle is considered.

INTRODUCTION

The goal of this study is to establish a time-efficient algorithm which will allow a planar 3R robot to reach a target point while avoiding a circular obstacle inside the workspace. It is required that the tip of the manipulator move along a straight line with a constant orientation of the end-effector. First, the Reachable Area (**RA**) of the wrist is determined when a circular obstacle is placed inside the workspace.

The present algorithm, which is based on the geometry of the manipulator and the location of obstacles, is different from the hierarchical approach developed by Udupa [1]. It is also different from the geometrical approach of Lumelsky [2] and the approach based on the artificial potential field by Khatib [3]. Other algorithms concerned with motion planning and obstacle avoidance using free space have been suggested by Perez [4,5] and Brooks [6]. More recently Young and Duffy [7,8] and Chen and Duffy [9,10] have comprehensively discussed the parallel operation of robots and interference avoidance motion planning.

REACHABLE AREA OF THE WRIST

The geometry for deriving the **RA** of the wrist [1] depends on the distance d between the center of the obstacle and the first joint of the robot, the dimension of the links, and the radius r of the obstacle. There are essentially three distinct cases which must be considered (see Fig.1):

Case (1): $d > a_{12} + (a_{23}^2+r^2)^{1/2}$. For this case link a_{23} cannot be tangent to the obstacle, and it follows that part of the arc of the obstacle which lies inside the circle C_{30} can be reached by the wrist point. Further, link a_{12} cannot touch the obstacle.

Case (2): $r + a_{12} < d \leq a_{12} + (a_{23}^2 + r^2)^{1/2}$. For this case link a_{23} is tangent to the obstacle and the obstacle lies outside the circle C_2. It follows that the part of the arc e_1e_2 of the obstacle which lies inside the circle C_{30} cannot be reached by the wrist point. Again link a_{12} cannot touch the obstacle.

Case (3): $r < d \leq r + a_{12}$. For this case either the obstacle intersects C_2 or the obstacle lies within C_2, and in either case link a_{12} can interfere with the obstacle during a specified motion. If this occurs, then obviously the motion is not possible.

---

[1] It is assumed throughout this analysis that the robot does not change its configuration viz. the algorithm is developed here for the robot in the elbow up position ($0 \leq \theta_2 \leq 180$ deg.). A similar algorithm can be easily developed for the elbow down position. These pair of algorithms form a basis for developing a further algorithm which makes use of the change of configuration to avoid obstacles.

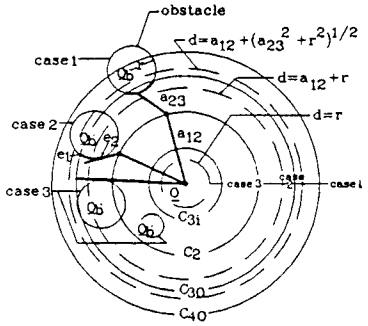

Fig.1 Determination of Cases (1), (2), and (3).

Computation of **RA** for Case (1)

The outer boundary of the workspace of the wrist (see Fig.2) is C_{3O}. The wrist cannot move in the three shaded areas (a), (b) and (c), which are denoted as Nonreachable Areas (**NA**)s of the wrist in the following discussion. **NA**(a) is defined by the central limit circle C_{3i} which is the inner boundary of the wrist point, and is represented by a logical variable

$$\overline{M}=(C_{3i}(\underline{X})<0) \ V \ [(L_4(\underline{X})<0)\wedge(K_4(\underline{X})<0)] = 1. \quad (1)$$

This equation shows that any point $\underline{X}$ inside **NA**(a) must lie either inside C_{3i} (for which $C_{3i}(\underline{X})<0$) or inside the area bounded by the pair of tangents K_4 from point 3 to the circle C_{3i}, the line L_4 through the points of tangency, and the arc of C_{3O} bounded by the tangents K_4. (see Lipkin, Torfason and Duffy [11]).

The **NA**(b) defined by the obstacle C_{ob} can be determined analogously by the logical variable

$$\overline{M}=(C_{ob}'(\underline{X})<0)V[(L_5'(\underline{X})<0)\wedge(K_5'(\underline{X})<0)] = 1. \quad (2)$$

Since the origin of the new coordinate system is shifted to $\underline{O}_b$ (the center of the obstacle), the tangents K_5 from point 3 to the obstacle and the line L_5 through points of tangency are denoted by K_5' and L_5' respectively.

Clearly, the outer annulus, **NA**(c), is inaccessible to the wrist, and the **RA** of the wrist can be determined by deleting these **NA**s from the wrist workspace. The derivations for the **NA**(a), **NA**(b), and **NA**(c) for Cases (2) and (3) are identical to Case (1). However, because the obstacle in Cases (2) and (3) is in different locations, additional further nonreachable zones must be computed.

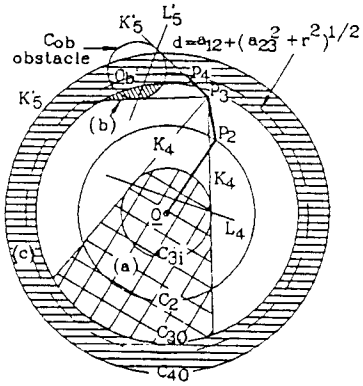

Fig.2 Determination of **NA**s (a), (b), and (c).

Computation of **RA** for Case (2)

In addition to the **NA**(a), **NA**(b), and **NA**(c), a further **NA** which cannot be reached by the wrist for the existence of a pair of coupler curves should be deleted from the wrist workspace (see Case (2.1) for more detail).

The analysis can be simplified by determining at the outset the position p_3 of the wrist point relative to the obstacle. This is accomplished by drawing three lines L_1, L_2, and L_3 which divide the workspace into three different zones (I), (II), and (III) (see Fig.3). L_1 is drawn from O and is tangent to the obstacle on the right side to the obstacle at point g_1 [2]. L_2 is tangent to the obstacle at point e and intersects circle C_2 at B [3] where eB = a_{23}. L_3 passes through the points of contact g_1 and e.

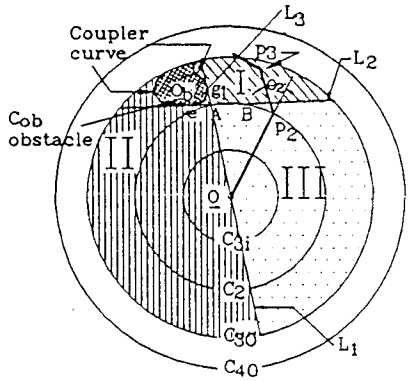

Fig.3 Determination of Zones (I), (II), and (III).

According to the location of the wrist point, three distinct situations are considered as follows.

Case (2.1): The wrist point p_3 is in zone(I) (see Fig.4). Suppose that joint 2 is initially coincident with A and link a_{23} is tangent to the obstacle. As joint 2 moves from A to B with a_{23} maintaining tangency, the wrist will trace a coupler curve from e_1 to e_4. This motion can be modeled by a planar RRRP mechanism (Duffy [12]). Points e_1, e_4 and two other intermediate points e_2 and e_3 are introduced and the coupler curve is approximated by the sequence of line segments $\underline{e_1e_2}$, $\underline{e_2e_3}$, and $\underline{e_3e_4}$. The points e_2 and e_3 are determined by choosing the points D_2 and D_3 on the arc AB, where $AD_3=D_3B$ and $AD_2=D_2D_3$. Point 3 is coincident with points e_2 and e_3, when joint 2 is coincident with points D_2 and

---

[2] Figure 4 is drawn for the robot in the elbow up position ($0\le\theta\le180$). If the robot was in the elbow down position ($-180\le\theta\le0$), the tangent line to a point g_1' on the left side would be used.

[3] If L_2 intersects the circle C_2 at two points, the intersection which is on the right hand side of the obstacle and eB = a_{23} is chosen. Further, if $d^2\le(a_{12}+r)^2+a_{23}^2$, it is preferable to use the line which is common tangent to both the obstacle and the circle C_2 as the line L_2.

D_3 and the link a_{23} is tangent to the obstacle.

Lines through $\underline{p}_3\underline{e}_1$, $\underline{p}_3\underline{e}_2$, $\underline{p}_3\underline{e}_3$ and $\underline{p}_3\underline{e}_4$ can now be drawn which divides the **NA** bounded by C_{30} and the line segments $\underline{e}_1\underline{e}_2$, $\underline{e}_2\underline{e}_3$ and $\underline{e}_3\underline{e}_4$ into three parts (s_1), (s_2) and (s_3). For convenience the lines through $\underline{p}_3\underline{e}_1$, $\underline{p}_3\underline{e}_2$ and $\underline{e}_1\underline{e}_2$ are labeled by N_4', N_5' and N_6'. A new coordinate system with origin $\underline{O}'$ is chosen on the midpoint of the ray through $\underline{p}_3$ which bisects $\underline{e}_1\underline{e}_2$, and

$$\underline{O}' = [\ 0.5 \times (\ \underline{e}_1 + \underline{e}_2\ ) + \underline{p}_3\ ] \times 0.5, \quad (3)$$

This choice ensures that any point within **NA**(s_1) is on the same side of $\underline{O}'$ as the lines N_4' and N_5' but on the opposite side of $\underline{O}'$ as the line N_6', which in turn facilitates the identification of points lying within the **NA**(s_1). Such points can be easily determined by the logical variable

$$\overline{M}=(N_4'(\underline{X})<0)\wedge(N_5'(\underline{X})<0)\wedge(N_6'(\underline{X})>0)=1. \quad (4)$$

Further, points in **NA**(s_2) and **NA**(s_3) can be identified using (3) and (4) by replacing (e_1,e_2) with (e_2,e_3) and (e_3,e_4) respectively.

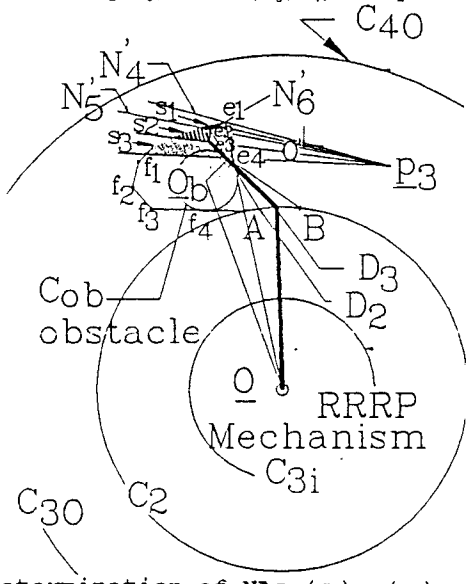

Fig.4 Determination of **NA**s (s_1), (s_2), and (s_3).

Case (2.2): The wrist point is in zone(II) (see Fig.5). This case is the same as Case (2.1) above. The points e_1, e_2, e_3 and e_4 are replaced by f_1, f_2, f_3 and f_4, and in this way equations (3) and (4) can be used to define the **NA**s.

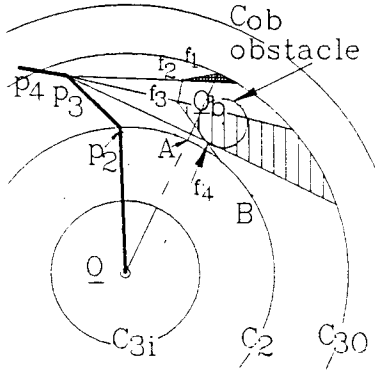

Fig.5 Determination of Case (2.2).

Case (2.3): The wrist point is in zone(III). The union of the **NA**s, which are determined from Cases (2.1) and (2.2), yields the **NA** for this case.

It remains to delete the **NA**s from the wrist workspace which will generate the **RA** of the wrist for Case (2).

Computation of **RA** for Case (3)

In addition to the **NA**(a), **NA**(b), and **NA**(c) computed in Case (1), several other **NA**s must be considered. In this case the wrist workspace is divided into two zones (I) and (II) by a line L_4 which passes through $\underline{O}_b$ and $\underline{O}$ (see Fig.6).

According to the locations of the wrist point and the obstacle, five distinct situations must be considered as follows.

Case (3.1): The wrist is in zone(I) and $(a_{12}^2+r^2)^{1/2}<d\leq a_{12}+r$. In this case, L_1 drawn from O is tangent to the obstacle on the right side at the point h_1 (see Fig.7) and intersects the circle C_2 at the point A, which is closest to the tangency h_1. And h_1 lies outside C_2. The derivation of the **NA** (t_1) and (t_2), which are bounded by the coupler curves e_2e_3 and e_4e_5, the rays from point 3, and the arc of C_{30}, is the same as that for Case (2.1).

The **NA**(t_3) is bounded by the circular arcs e_1e_2 and e_6e_7, and by the lines L_5', L_6' and L_7' through $\underline{p}_3\underline{e}_2$, $\underline{p}_3\underline{e}_1$ and $\underline{e}_1\underline{e}_2$. A new coordinate system with the origin $\underline{O}'$ is chosen on the midpoint of the ray through p_3 which bisects $\underline{e}_1\underline{e}_2$, and

$$\underline{O}' = (\ 0.5 \times (\ \underline{e}_1 + \underline{e}_2\ ) + \underline{p}_3\ ) \times 0.5. \quad (5)$$

This choice ensures that any point X within **NA**(t_3) is on the same side of $\underline{O}'$ as lines L_5' and L_6' but on the opposite side of $\underline{O}'$ as the line L_7'. Further, it ensures that the distance from the point X to the point A must be greater than a_{23}, i.e., that is $XA>a_{23}$. This in turn facilitates the identification of points lying within the **NA**(t_3). Such points can be easily determined by a logical variable

$$\overline{M}=(XA>a_{23})\wedge(L_5'(\underline{X})<0)\wedge(L_6'(\underline{X})<0)\wedge(L_7'(\underline{X})>0)=1, \quad (6)$$

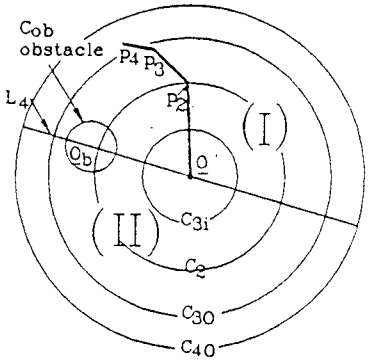

Fig.6 Determination of Zones (I) and (II) in Case (3).

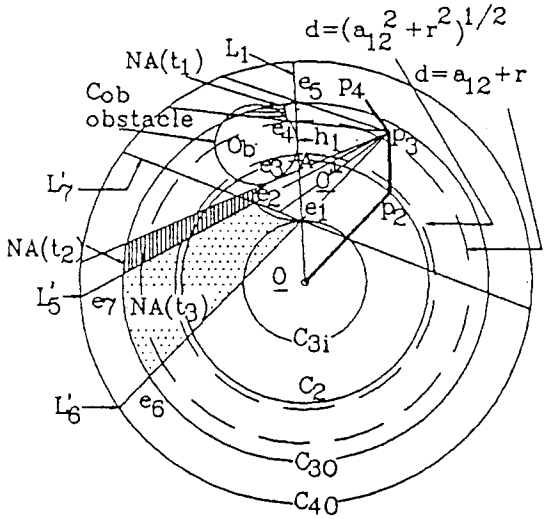

Fig.7 Determination of **NA**s (t_1), (t_2), and (t_3).

Case (3.2): The wrist is in zone(I) and $(a_{12}-a_{23})^2+r^2<d^2\leq(a_{12}^2+r^2)$. In this case, L_1 is drawn from O and is tangent to the obstacle on the right side at point h_2 (see Fig.8). Here h_2 lies between C_2 and C_{3i}. The circular arc e_1e_2, the two coupler curves e_2e_3 and e_4e_5, and the circle C_{3O} together with the rays from point 3 bound and divide the **NA** into three parts (u_1), (u_2) and (u_3). The derivation of the **NA**(u_i), **NA**(u_2) and **NA**(u_3) is the same as that in Case (3.1). However, the location of **NA**(u_1) is different from that of **NA**(t_3) shown in Fig.7.

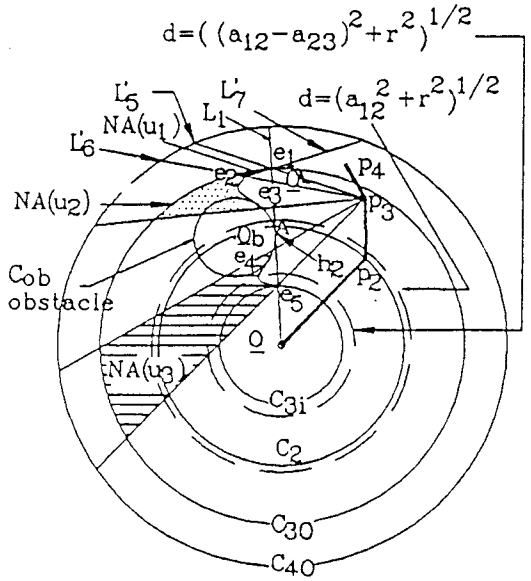

Fig.8 Determination of the **NA**s of Case (3.2).

Case (3.3): The wrist is in zone(I) and $r<d\leq((a_{12}-a_{23})^2+r^2)^{1/2}$. In this case, L_1' is drawn from O and is tangent to the obstacle on the right side at point h_3, and point h_3 lies inside C_{3i}. The **NA** (see Fig.9) is bounded by the arc of the circle C_{3O}, the semicircle e_1e_2, and the lines L_8' and L_9' through $\underline{p_3e_1}$ and $\underline{p_3e_2}$. The center of the semicircle is at point A and the radius is a_{23}. Three figures are drawn separately in order to identified **NA**(v_1), **NA**(v_2) and **NA**(v_3) which are defined by the different locations of the wrist point p_3.

When the wrist point is outside the area bounded by the semicircle e_1e_2 and the line L_1' (see Fig.9(a)), the **NA**(v_1) is defined by

$$\bar{M}=(XA>a_{23})\wedge(L_8'(\underline{X})<0)\wedge(L_9'(\underline{X})<0)\wedge(L_1'(\underline{X})>0)=1. \quad (7)$$

The origin of the new coordinate system is given by $\underline{O}'=0.5x(0.5x(\underline{e_1}+\underline{e_2})+\underline{p_3})$. Equation (7) is identical to equation (6) with lines L_5', L_6' and L_7' replaced by L_8', L_9' and L_1'.

If the wrist is inside the semicircular area (see Fig.9(b)), the **NA**(v_2) is bounded by C_{3O}, the semicircle e_1e_2 and lines L_8' and L_9' through $\underline{p_3e_1}$ and $\underline{p_3e_2}$. A new coordinate system with origin $\underline{O}'$ is chosen on the midpoint of the ray through p_3 which bisects $\underline{e_1e_2}$, and $\underline{O}'=0.5x(0.5x(\underline{e_1}+\underline{e_2})+\underline{p_3})$. This choice ensures that any point X within **NA**(v_2) is on the opposite side of $\underline{O}'$ as lines L_8' or L_9', and the distance from the point X to the point A is greater than a_{23}, that is $XA>a_{23}$. This in turn facilitates the identification of points lying within the **NA**(v_2). Such points can be defined by a logical variable

$$\bar{M}=(XA>a_{23})\wedge[(L_8'(\underline{X})>0)\vee(L_9'(\underline{X})>0)]=1. \quad (8)$$

If the wrist is exactly on line L_1' (see Fig.9(c)), the origin is shifted from $\underline{O}$ to $\underline{O_b}$. The **NA**(v_3) is bounded by C_{3O}, the semicircle e_1e_2 and the line L_1'. The origin of the new coordinate system is shifted to $\underline{O_b}$ so as to ensure that any point within **NA**(v_3) is on the same side of $\underline{O_b}$ as line L_1', and the distance from the point to the point A is greater than a_{23}, that is $XA>a_{23}$, which in turn facilitates the identification of points lying within the **NA**(v_3). Such points can be defined by

$$\bar{M}=(XA>a_{23})\wedge(L_1'(\underline{X})<0)=1, \quad (9)$$

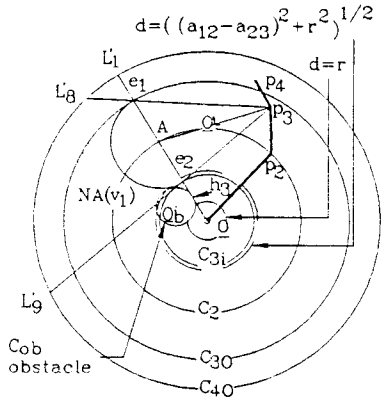

Fig.9a Determination of **NA** (v_1).

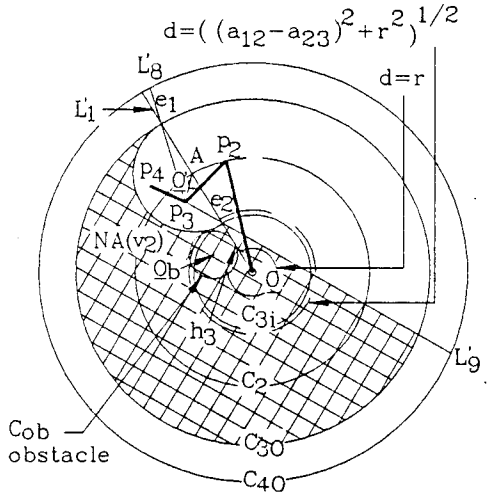

Fig.9b Determination of NA (v_2).

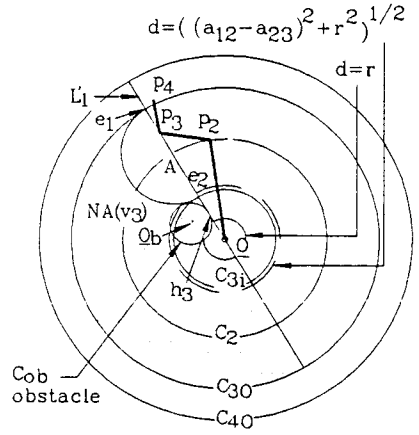

Fig.9c Determination of NA (v_3).

Case (3.4): The wrist is in zone(II) and $(a_{12}^2+r^2)^{1/2}<d\le a_{12}+r$. In this case, L_1 is drawn from O and is tangent to the obstacle on the left side at point h_4 (see Fig.10). And h_4 lies outside the circle C_2. L_1 intersects the circle C_{3i}, C_2, and C_{3O} at the points e_3, A, and e_1 respectively, which are closest to the tangent point h_4. It is convenient to determine the **NA** by introducing a virtual obstacle C_{obv}', whose center is g_3 [4] and radius is g_3e_1.

The **NA** bounded by C_{obv}', the tangents K_{obv}' from point 3 to the virtual obstacle, and the line L_{obv}' through points of tangency is defined by a logical variable

$$\bar{M}=(C_{obv}'(\underline{X})<0)\vee[(L_{obv}'(\underline{X})<0)\wedge(K_{obv}'(\underline{X})<0)]=1, \quad (10)$$

where the origin of the new coordinate system is shifted to g_3. Equation (10) is the same as equation (1) with C_{3i}, L_4 and K_4 replaced by C_{obv}', L_{obv}' and K_{obv}'.

[4] Circle C_2 intersects the obstacle C_{ob} at two points, and the intersection which is nearest to the point h_4 is chosen to be point g_3.

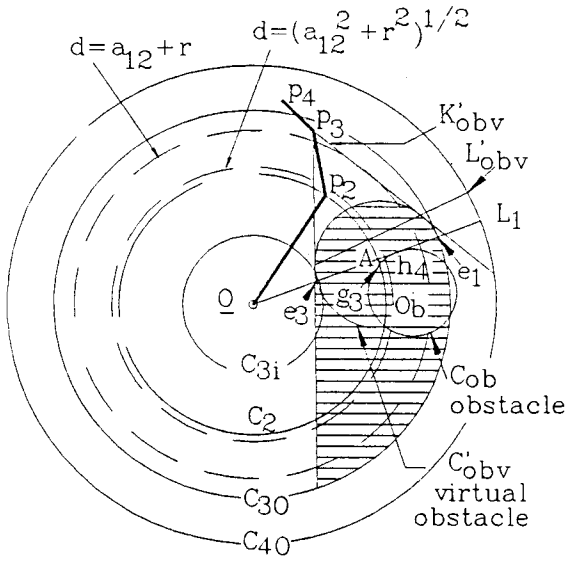

Fig.10 Determination of the NA of Case (3.4).

Case (3.5): The wrist is in zone(II) and $r<d\le(a_{12}^2+r^2)^{1/2}$. In this case, L_1 is drawn from O and is tangent to the obstacle on the left side at point h_5. And point h_5 lies inside the circle C_2 (Fig.11). L_1 intersects the circle C_{3i}, C_2, and C_{3O} at the points e_3, A, and e_1 respectively, which are nearest to the tangent point h_5. The **NA** of this case can be determined by introducing a virtual obstacle C_{obv}', the tangents K_{obv}' from point 3 to C_{obv}', and the line L_{obv}' through points of tangency. The center of C_{obv}' is at point A and the radius is a_{23}. Hence equation(10) can be used again to determine the **NA**.

It remains to delete the NAs from the wrist workspace which will generate the **RA** of the wrist.

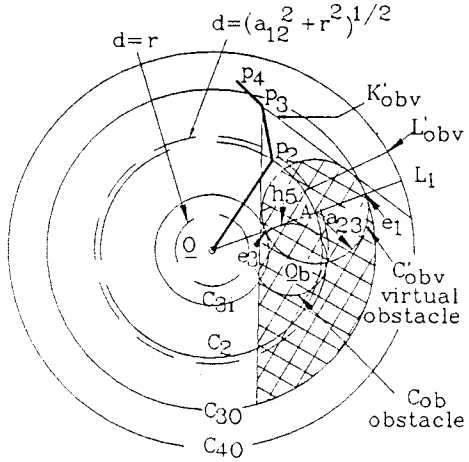

Fig.11 Determination of the NA of Case (3.5).

CONCLUSION

In this paper, workspace geometry is employed to determine the motion capability of the wrist point of a planar 3R manipulator with a circular obstacle inside the workspace. This

constitutes the foundation for determining the Reachable Area of a point in the end effector. Following this procedure an algorithm is developed for determining a free path of a planar 3R manipulator to avoid a single circular obstacle and subsequently multiple circular obstacles.

ACKNOWLEDGEMENT

The authors wish to acknowledge the financial support of the Department of Energy (Grant No. DE-FG02-86NE37967).

REFERENCES

1. Udupa S. M., "Collision Detection And Avoidance In Computer Controlled Manipulators," Fifth International Joint Conference on Artificial Intelligence, MIT, Cambridge, Massachusetts, August 1977, pp. 737-748.

2. Lumelsky V. J., "On Non-Heuristic Motion Planning In Unknown Environment,"IFAC Symposium on Robot Control (SYROCO'85), Barcelona, Spain, November 1985, pp. 737-748.

3. Khatib Oussama, "Real-Time Obstacle Avoidance for Manipulators and Mobile Robots, "IEEE 1985 International Conference on Robotics and Automation, St. Louis, Missouri, March 25-28 1985, pp. 500-505.

4. Lozano-Perez Tomas, "Task Planning, "Robot Motion, The MIT Press Series in Artificial Intelligence, Cambridge, Massachusetts, 1982, pp. 473-498.

5. Lozano-Perez Tomas, "Automatic Planning of Manipulator Transfer Movements," Robot Motion, The MIT Press Series in Artificial Intelligence, Cambridge, Massachusetts, 1982, pp. 499-535.

6. Brooks R.A., "Planning Collision Free Motions for Pick and Place Operations," The First International Robotics Research Symposium, The MIT Press, Cambridge, Massachusetts, 1984, pp. 5-38.

7. Young L. and Duffy J., "A Theory for the Articulation of Planar Robots: Part I - Kinematic Analysis for the Flexure and the Parallel Operation of Robots," Design Engineering Technical Conference, October 5-8, Columbus, Ohio, 1986.

8. Young L. and Duffy J., "A Theory for the Articulation of Planar Robots: Part II - Motion Planning Procedure for Interference Avoidance," Design Engineering Technical Conference, October 5-8,Columbus, Ohio, 1986.

9. Chen, J.L. and Duffy, J., "An Analysis for Rectilinear Parallel Operation of a Pair of Spatial Manipulators: Part I - Motion Capability," Trends and Developments in Mechanisms, Machines, and Robotics-1988, Vol. 3, Sept. 1988, pp. 393-400.

10. Chen, J.L. and Duffy, J., "An Analysis for Rectilinear Parallel Operation of a Pair of Spatial Manipulators: Part II - Range of End Effector Orientation," Trends and Developments in Mechanisms, Machines, Robotics-1988, Vol. 3, Sept. 1988, pp. 393-400.

11. Lipkin H., Torfason L. E., and Duffy J., "Efficient Motion Planning for a Planar Manipulator Based on Dexterity and Workspace Geometry," Conference on Mechanisms and Machinery, Cranfield Institute of Technology, Cranfield, United Kingdom, September 1985.

12. Duffy J., "Planar Mechanisms and Manipulators", Analysis of Mechanisms and Robot Manipulators, Wiley, New York, 1980, pp. 5-55.